Article ID: 1007-7294(2024)12-1803-17

A Framework of LSTM Neural Network Model in Multi-Time Scale Real-Time Prediction of Ship Motions in Head Waves

CHEN Zhan-yang[1,2], *ZHAN Zheng-yong*[3], *CHANG Shao-ping*[3], *XU Shao-feng*[3], *LIU Xing-yun*[1]

(1. Department of Ocean Engineering, Harbin Institute of Technology at Weihai, Weihai 264209, China;
2. State Key Laboratory of Structural Analysis, Optimization and CAE Software for Industrial Equipment, Dalian University of Technology, Dalian 116024, China; 3. Flight Control System Department, AVIC Xi'an Flight Automatic Control Research Institute, Xi'an 710065, China)

Abstract: Ship motions induced by waves have a significant impact on the efficiency and safety of offshore operations. Real-time prediction of ship motions in the next few seconds plays a crucial role in performing sensitive activities. However, the obvious memory effect of ship motion time series brings certain difficulty to rapid and accurate prediction. Therefore, a real-time framework based on the Long-Short Term Memory (LSTM) neural network model is proposed to predict ship motions in regular and irregular head waves. A 15000 TEU container ship model is employed to illustrate the proposed framework. The numerical implementation and the real-time ship motion prediction in irregular head waves corresponding to the different time scales are carried out based on the container ship model. The related experimental data were employed to verify the numerical simulation results. The results show that the proposed method is more robust than the classical extreme short-term prediction method based on potential flow theory in the prediction of nonlinear ship motions.

Key words: deep learning; LSTM; ship motion; real-time prediction; irregular waves

CLC number: U661.32 **Document code:** A **doi:** 10.3969/j.issn.1007-7294.2024.12.001

0 Introduction

The large-amplitude motions of a ship in severe sea states endanger the maritime operational efficiency and safety, especially for special maritime operations such as ship-borne helicopter landing[1], ship-based missile launch and control of ship navigation in waves[2]. The determination of ship motions in the coming seconds can provide a decision-making basis for decision-makers to prevent and reduce the occurrence of accidents. Thus, real-time prediction of the deterministic ship motions has always been a hot issue in the hydrodynamic field.

By definition, the real-time prediction of ship motions is to achieve an accurate prediction of ship motions in the next few seconds, tens of seconds or even minutes by the rapid analysis and processing of the

Received date: 2024-06-21

Foundation item: Supported by Shandong Provincial Natural Science Foundation (ZR2024ME139); Aeronautical Science Foundation of China (2024M074189001); The Open Fund of State Key Laboratory of Structural Analysis, Optimization and CAE Software for Industrial Equipment, Dalian University of Technology (GZ23112)

Biography: CHEN Zhan-yang (1984-), male, Ph.D., associate professor, corresponding author, E-mail: chen_1228@163.com.

known data set. Then, the prediction results are applied in the operation guidance and compensation control of special maritime operations. In recent years, the extreme short-term prediction method of ship motions has been extensively studied in various subjects for its feature of immediacy.

As is known, the real wave environment is of irregular waves, and the significant wave height is an important parameter to represent the characteristics of ocean waves. Early studies on the prediction of significant wave height were developed based on the linear prediction model[3-5] and the classic time series prediction model[6-7]. These methods are applicable to the linear and stationary time series model. However, the time series model in high sea states is so complex with the characteristic of nonlinearity and nonstationarity. Thus, the performances of these methods are far from expected[8].

Fortunately, the machine learning approach provides a potential way for nonlinear ship motions prediction for its capability in nonlinearity processing. With the development of computer engineering, a large number of deep learning models and artificial intelligence technology have been introduced into the field of ship motion prediction, which includes the fuzzy mathematics method[9], chaos theory method[10] and neural network method[11-12], etc.. Furthermore, it has been confirmed that the neural network method shows excellent behavior in nonlinearity processing.

Recurrent Neural Network (RNN), a common neural network method, was designed to solve time sequence modeling problems. However, researchers found that when RNN model is used to predict ship motions in waves, then the training efficiency of the model will decrease, even leading to the gradient explosion and gradient vanishing. The primary reason is that the memory length is too long[13-14]. Gers et al pointed out that the forget gate of the LSTM model can avoid the gradient vanishing caused by the continuous product in solving the weight matrix gradient[15]. As is known, the motion time series of marine structure have obvious memory effect. In other words, the waves generated by the present motions will remarkably affect subsequent ship motions. Thus, the machine learning based LSTM model has been extensively employed in the time series modeling problems of marine structure motions.

By using the LSTM model, Qiao et al predicted the dynamic responses of mooring lines based on the ship motions. The results show that the mooring line responses predicted based on the LSTM model show high precision[16]. Sun et al proposed a new hybrid prediction model for ship motion attitude with LSTM neural network model and Gaussian Process Regression (GPR). The prediction experiments of ship rolling and pitch motions were carried out based on the proposed model, then the effectiveness and advancement of the hybrid model were verified[17]. Guo et al carried out the deterministic predictions of the heave motion of a floating semi-submersible, then quantified its uncertainty of the predictive time series[18].

The paper aims to achieve the real-time prediction of nonlinear ship motions in the coming seconds based on the past ship motion records. The structure of the paper is organized as follows: In chapter 1, the hydrodynamic formulations based on potential flow theory for nonlinear ship motions in regular and irregular waves are presented. Chapter 2 describes the implementation details of the LSTM neural networks. In Chapter 3, the numerical simulation verification and towing tank test verification are carried out in regular waves. Furthermore, the results corresponding to the different time scales in irregular waves are presented and discussed. Finally, Chapter 4 summarizes the work of this paper and gives the conclusions.

1 Hydrodynamic methods in the framework of potential flow theory

The ship motions in waves can be treated as a forced vibration under the wave excitation,

$$[\boldsymbol{a}]\{\ddot{\boldsymbol{\eta}}_r(t)\} = \{\boldsymbol{F}(t)\} \tag{1}$$

where, $[\boldsymbol{a}]$ denotes generalized structural mass matrix, $\{\boldsymbol{\eta}_r(t)\}$ denotes the rigid ship motions in waves, $r = 1, 2, \ldots, 6$ denotes the rigid modes for hydrodynamic analysis of rigid motions and $r \geqslant 7$ denotes the elastic modes for hydroelastic analysis, $\{\boldsymbol{F}(t)\}$ denotes all the fluid forces that include the hydrostatic restoring force, incident wave force, diffraction wave force, radiation force and slamming force.

1.1 Fluid forces

1.1.1 Hydrostatic restoring force

Differing from the linear theory, the nonlinear hydrodynamic theory takes into account the instantaneous wetted surface $S(t)$ and the slamming forces. Thus, the hydrostatic restoring force on instantaneous wetted surface $S(t)$ is calculated as follows:

$$\{\boldsymbol{F}_S^{(3)}\} = -\rho g \iint_{S(t)} \left(\{\boldsymbol{\eta}_3(t)\} - \{\boldsymbol{\eta}_5(t)\} x\right) n_3 \mathrm{d}s \tag{2}$$

$$\{\boldsymbol{F}_S^{(4)}\} = -\rho g \iint_{S(t)} y \{\boldsymbol{\eta}_4(t)\} n_4 \mathrm{d}s \tag{3}$$

$$\{\boldsymbol{F}_S^{(5)}\} = -\rho g \iint_{S(t)} (\boldsymbol{\eta}_3(t) - \boldsymbol{\eta}_5(t) \cdot x) n_5 \mathrm{d}s \tag{4}$$

where, ρ is the fluid density, $\{\boldsymbol{\eta}_3(t)\}$, $\{\boldsymbol{\eta}_4(t)\}$ and $\{\boldsymbol{\eta}_5(t)\}$ are the motion amplitudes of heave, rolling and pitch at time t respectively, $\vec{n} = (n_1, n_2, n_3)$ denotes the unit inner normal vector of the hull surface, perpendicular to the ship surface and pointing towards the interior of ship. And $(n_4, n_5, n_6) = (\vec{r} \times \vec{n})$, in which $\vec{r}$ is radius vector.

1.1.2 Wave exciting force

The wave exciting force of ships includes incident wave force and diffraction wave force. The incident force and diffraction force in regular waves can be written as by using the interception of instantaneous grid:

$$\begin{cases} \{\boldsymbol{F}_{\mathrm{I}}(t)\} = -\rho\zeta_a \iint_{S(t)} \vec{n}_r (\mathrm{i}\omega - U\dfrac{\partial}{\partial x}) \varphi_0 \mathrm{d}s \\ \{\boldsymbol{F}_{\mathrm{D}}(t)\} = -\rho\zeta_a \iint_{S(t)} \vec{n}_r (\mathrm{i}\omega - U\dfrac{\partial}{\partial x}) \varphi_d \mathrm{d}s \end{cases} \tag{5}$$

where, ζ_a is the wave amplitude of regular wave, ω is the wave frequency, φ_0 and φ_d are instantaneous incident potential and diffraction potential corresponding to unit wave amplitude.

To study the impact of different wave frequency components on the motion responses in irregular waves, the convolution relationship proposed by Cummins is used to obtain the incident wave force and diffraction wave force in irregular waves[19]:

$$\begin{cases} \{\boldsymbol{F}_{\mathrm{I}}(t)\} = \int_0^t h_r^{\mathrm{I}}(t-\tau)\zeta(\tau)\mathrm{d}\tau \\ \{\boldsymbol{F}_{\mathrm{D}}(t)\} = \int_0^t h_r^{\mathrm{D}}(t-\tau)\zeta(\tau)\mathrm{d}\tau \end{cases} \tag{6}$$

where, $\zeta(\tau)$ is the wave elevation at instant time of irregular waves, $h_r^{\mathrm{I}}(t)$and $h_r^{\mathrm{D}}(t)$ are the impulsive response function of incident wave force and diffraction wave force.

1.1.3 Radiation force

The memory effect of ship motion time series is related to the radiated waves. The significance of memory effect is that the present ship motion is related to the past ship motions. Thus, the memory effect needs to be considered in solving the radiation force. In this work, the time-domain memory function is used for the radiation force in irregular waves:

$$\left\{\boldsymbol{F}_{\mathrm{R}}(t)\right\} = -\left[\boldsymbol{\mu}(\infty)\right]\left\{\ddot{\boldsymbol{\eta}}_r(t)\right\} - \int_0^{\infty}\left[\boldsymbol{K}(\tau)\right]\left\{\dot{\boldsymbol{\eta}}_r(t-\tau)\right\}\mathrm{d}\tau \tag{7}$$

where, $\left[\boldsymbol{\mu}(\infty)\right]$ is the added mass as $\omega \to \infty$. $\left[\boldsymbol{K}(\tau)\right]$ is the memory function.

As for the regular wave with single frequency, the radiation force in irregular waves can be reduced to the expression as follows:

$$\left\{\boldsymbol{F}_{\mathrm{R}}(t)\right\} = -[\boldsymbol{A}(\omega)]\left\{\ddot{\boldsymbol{\eta}}_r(t)\right\} - [\boldsymbol{B}(\omega)]\left\{\dot{\boldsymbol{\eta}}_r(t)\right\} \tag{8}$$

where, $[\boldsymbol{A}(\omega)]$ is the added mass with frequency ω, $[\boldsymbol{B}(\omega)]$ is the fluid damping coefficient with frequency ω, both of which are 6×6 matrices. In this work, a semi-analytical method proposed by Cao for $\left[\boldsymbol{K}(\tau)\right]$ in the whole frequency range is employed[20].

1.1.4 Slamming force

In this work, the momentum slamming theory is applied to predicted slamming loads:

$$\left\{\boldsymbol{F}_f(\boldsymbol{x},\boldsymbol{t})\right\} = \begin{cases} \dfrac{\mathrm{d}m(x,t)}{\mathrm{d}z}\left(\dfrac{\mathrm{d}Z_R}{\mathrm{d}t}\right)^2 & \dfrac{\mathrm{d}Z_R}{\mathrm{d}t} < 0 \\ 0 & \dfrac{\mathrm{d}Z_R}{\mathrm{d}t} > 0 \end{cases} \tag{9}$$

where, $m(x, t)$ is the instantaneous added mass, and $Z_R(x, t)$ is the vertical relative ship motion to wave in vertical plane.

1.2 Hydrodynamic time-domain motion equation

When the above fluid forces acting on the hull are obtained, the hydrodynamic motion equation at each instant time in regular and irregular waves can be expressed as follows:

$$\begin{aligned} &\left(\left[\boldsymbol{a}\right] + \left[\boldsymbol{\mu}(\infty)\right]\right)\left\{\ddot{\boldsymbol{\eta}}_r(t)\right\} + \int_0^t [\boldsymbol{K}(\tau)]\left\{\dot{\boldsymbol{\eta}}_r(t-\tau)\right\}\mathrm{d}\tau + [\boldsymbol{C}]\left\{\boldsymbol{\eta}_r(t)\right\} \\ &\quad = \left\{\boldsymbol{F}_{\mathrm{I}}(t)\right\} + \left\{\boldsymbol{F}_{\mathrm{D}}(t)\right\} + \left\{\boldsymbol{F}_{\mathrm{f}}(t)\right\} \end{aligned} \tag{10}$$

Finally, the fourth-order Runge-Kutta method and modal superposition method are adopted to predict the 6-degree ship motions at each time step.

2 LSTM neural network

2.1 Basic concepts of LSTM model

Due to the excellent performance in time series prediction, LSTM has been applied in the long sequence training, such as time-domain prediction of ship motions[17, 21-22]. As a special RNN model,

the LSTM cell contains three gates to control the cell state, which are forget gate, input gate and output gate. The LSTM cell structure is shown in Fig.1.

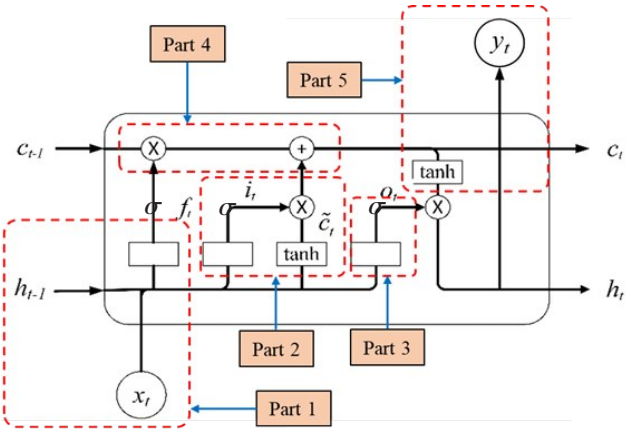

Fig.1 Internal structure of LSTM model

As shown in Fig.1, the internal structure of LSTM model includes 5 parts. Part 1 is the forget gate f_t, which determines the information discarded from the previous cell. The calculation process can be expressed as:

$$f_t = \sigma\left(W_f \cdot \begin{bmatrix} h_{t-1} \\ x_t \end{bmatrix} + b_f\right) \tag{11}$$

where, x_t, h_{t-1}, W_f and b_f represent the present input, the previous hidden state, the weight matrix of forget gate and offset vector of forget gate, respectively.

Part 2 is the input gate i_t, which determines the information added to the current cell. The calculation process can be expressed as:

$$i_t = \sigma\left(W_i \cdot \begin{bmatrix} h_{t-1} \\ x_t \end{bmatrix} + b_i\right) \tag{12}$$

$$\tilde{c}_t = \tanh(W_c \cdot [h_{t-1}, x_t] + b_c) \tag{13}$$

where, W_i and b_i represent the weight matrix and offset vector of input gate, $\tilde{c}_t$ is the temporary state, W_c and b_c represent the weight matrix and offset vector of the current cell state. σ and tanh are the activation functions, their calculation formulas are as follows:

$$\sigma(x) = \frac{1}{1 + e^{-x}} \tag{14}$$

$$\tanh(x) = \frac{e^{x} - e^{-x}}{e^{x} + e^{-x}} \tag{15}$$

Part 3 is the output gate o_t, which determines the information exported from the current cell. The calculation process can be expressed as:

$$o_t = \sigma\left(W_o \cdot \begin{bmatrix} h_{t-1} \\ x_t \end{bmatrix} + b_o\right) \tag{16}$$

where, W_o and b_o represent the weight matrix and offset vector of output gate, respectively.

Part 4 is the update structure of the current cell state, which is used to remember the input of the previous moment for neurons. In the process of data transmission, the current cell state c_t can be obtained by the previous cell state c_{t-1} and temporary state $\tilde{c}_t$.

$$c_t = f_t \cdot c_{t-1} + i_t \cdot \tilde{c}_t \tag{17}$$

It should be mentioned that the information of the current cell state c_t does not copy the previous cell state c_{t-1} completely, but chooses to forget some content and remember some new content based on c_{t-1}. As shown in Eq.(17), the relationship between the previous cell state and the current cell state is not a composite function, but a linear superposition of multiple independent functions. This means that the likelihood of gradient explosion and gradient vanishing will be greatly reduced.

Part 5 is the output information of the current cell state C_t, which is used to output the final learning results. The current hidden state h_t can be expressed as:

$$h_t = o_t \cdot \tanh(c_t) \tag{18}$$

Once the LSTM model achieves the sequence feature extraction, the features would be input into a fully connected layer to calculate the final output of the whole neural network, which is shown as follows:

$$y_t = \phi\left(W_y h + b_y\right) \tag{19}$$

where, y_t denotes all the predicted future ship motions, W_y and b_y represent the weight matrix and offset vector of predicted future ship motions.

2.2 Principle of prediction of ship motion based on LSTM model

The LSTM model can be regarded as a complex unknown function. The past motion data of a ship, which can be taken as independent variable, is imported into the function to train LSTM model and adjust parameters continuously. Thus, the basis for predicting future ship motions is to build an LSTM model by programming. Firstly, the known ship motion data are imported to train the model. Then, the model parameters are adjusted in each iteration so that the rule of data change can be learnt and recorded by the model. Finally, the ship motion data in the coming seconds can be predicted based on the trained LSTM model.

Taking the simple linear regression model as an example, the essence of prediction of future data is explained as follows. Generally speaking, Eq.(20) is selected to fit a series of data to obtain future predicted values.

$$f_{w,b}(x) = wx + b \tag{20}$$

where, x is the input variable, and $f_{w,b}(x)$ is the predicting function. During the training process, both $f(x)$ and x are known values, w and b are the undetermined parameters of the regression model. Thus, the purpose of training is to fit the undetermined parameters of the model. During the testing, w and b have been trained to reach the optimal value, Then the future ship motions can be predicted by $f(x)$.

The loss function, which is the mean square error, can be obtained by the training set.

$$L(w,b) = \frac{1}{2m}\sum_{i=1}^{m}\left(f_{w,b}^{(i)}(x) - y^{(i)}\right)^2 = \frac{1}{2m}\sum_{i=1}^{m}\left(wx^{(i)} + b - y^{(i)}\right)^2 \tag{21}$$

where, y is the output variables, that is, the true values. And m is the total number of training samples, $\left(x^{(i)}, y^{(i)}\right)$ is the i–th training sample, $f_{w,b}^{(i)}(x)$ is the value obtained by substituting $x^{(i)}$ into function $f(x)$. Given that the loss function is the mean squared error, a smaller value of the loss function implies a higher degree of model to fit the data.

Substituting the loss function into the gradient descent formula, the iterative expression for the

undetermined parameters in regression models can be derived, as shown in Eq.(22):

$$\begin{cases} w^{(j+1)} = w^{(j)} - \alpha \dfrac{\partial}{\partial w} L\left(w^{(j)}, b^{(j)}\right) = w^{(j)} - \alpha \dfrac{1}{m} \sum_{i=1}^{m} \left(w^{(j)} x^{(i)} + b^{(j)} - y^{(i)}\right) x^{(i)} \\ b^{(j+1)} = b^{(j)} - \alpha \dfrac{\partial}{\partial b} L\left(w^{(j)}, b^{(j)}\right) = b^{(j)} - \alpha \dfrac{1}{m} \sum_{i=1}^{m} \left(w^{(j)} x^{(i)} + b^{(j)} - y^{(i)}\right) \end{cases} \tag{22}$$

where, $w^{(j)}$ and $b^{(j)}$ are the values of the undetermined parameters of the model at present, $w^{(j+1)}$ and $b^{(j+1)}$ are the updated parameter values of the model after the next gradient descent, α is the learning rate which can controls the speed of parameter changing with gradient.

The role of known data in the training of model parameters can be intuitively demonstrated by Eq.(22). The model can be trained by substituting the known input variables and the corresponding output variables. It is noted that in each cycle, both w and b need to be updated simultaneously to obtain the correct model parameters. After certain data or cycles, the appropriate model parameters w and b can be obtained with the minimum value of the loss function. At this point, the model can have good ability to fit data. Then the corresponding output variable results y can be obtained by substituting the unknown input variable values x into the model.

The procedure of predicting data based on the LSTM model is similar to the above example. Differing from the linear regression model, the LSTM model is more complex and have more connection layers. The process of predicting ship motion data based on LSTM model is shown in Fig.2.

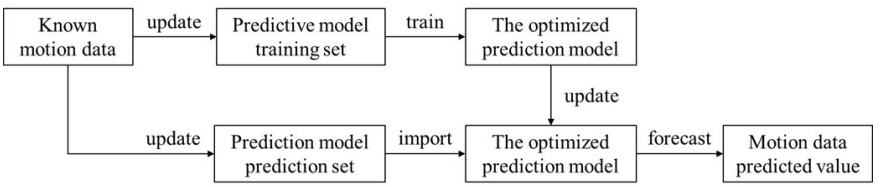

Fig.2 LSTM model prediction process

2.3 Set-up and training of LSTM model

In this work, the LSTM neural network model is built, trained and tested based on the TensorFlow platform. Firstly, the computational neuron units are established, and then these neurons are connected into hidden layer units. Secondly, according to the calculation requirements, the hidden layer is copied and connected into hidden layer structure. Finally, the corresponding parameters are configured to complete the construction of LSTM neural network framework. The LSTM neural network layers are shown in Fig.3.

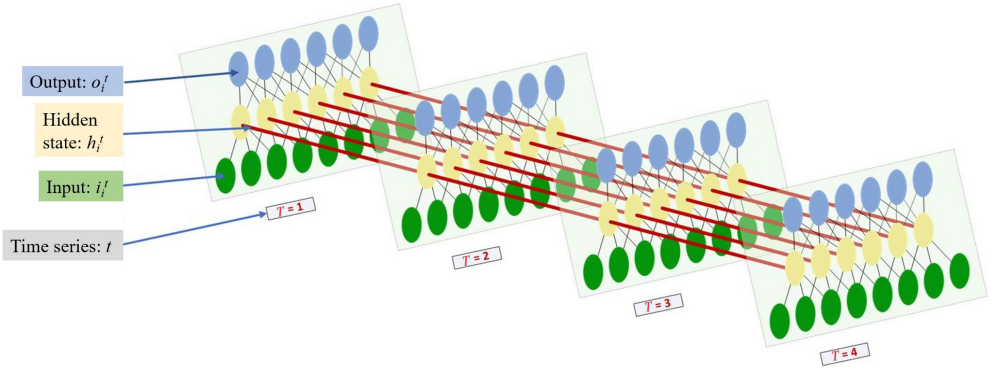

Fig.3 LSTM neural network layers

The computer environment and software version for building the LSTM model are listed as follows:

- Operating System: Win10;
- Graphics Card: NVIDIA Quadro RTX 6000;
- Visual Studio: 2019;
- CUDA: 10.0;
- cuDNN: 10.0;
- Anaconda Environment Manager: 64 bit;
- Packages: Python 3.8;
- TensorFlow: 2.0.

Firstly, the hyper-parameters (such as input_size, hidden_size, num_layers, output_size), which can directly affect the structure of the LSTM model, are set for the LSTM model. Then the dataset needs to be preprocessed and divided into training and test sets. Secondly, LSTM model structure is defined, including assigning values to hyper-parameters, selecting activation function, etc. After the preparation work is completed, the LSTM model is trained and the training set is imported for iterative loop. By reducing the value of the loss function continuously, the fitting degree of the model to the data is gradually improved. Finally, when the training frequency reaches the target value, the training process is completed, and the model parameters are saved so that the updated model parameters can be used directly for the predicton of ship motion. When predicting the actual ship motion data, only the trained model parameters need to be imported to predict the future motions based on the existing data.

The prediction accuracy mainly depends on the training effect of the model, which is determined by the input-output pairs of the training sets. It is worth noting that when the ship is operating at sea, it is usually equipped with a motion measurement device in order to transmit the ship motion data to the shipboard aircraft. Differing from the traditional real-time prediction method that takes wave height as input and ship motions as output, the data of obtained past ship motions are defined as the original input values, and the data of ship motions in the coming seconds are defined as the original output values in this work. The ship motion responses in head waves refer to the heave and pitch motions of the ship in regular and irregular waves. To improve the training effect of the model, the input-output pairs of training sets should cover all possible sea states, and the data need to be evenly distributed in the range of possible sea states. The training data are obtained based on the 3-D nonlinear hydrodynamic method presented in Chapter 1.

The initialization neuron parameters of the LSTM model are randomly generated, which is the same as all deep learning models. The Back Propagation Through Time (BPTT) algorithm is applied for the reverse solution of the gradient, and then the model neurons parameters are adjusted according to the gradient until convergence[23]. More details about the BPTT algorithm are presented in the work of Guo et al[22]. In this work, the corresponding parameters of LSTM model in the framework of TensorFlow are:

- Activation function: tanh;

•Optimizer: Adam;
•Learning rate: 0.000 5;
•Reuse variable: True.

3 Results and discussion

3.1 Method validation in regular waves

In addition to the training set of LSTM neural network model, the validating set, which is used for validating the accuracy of the predicting results from the trained LSTM neural network model, should also be given. Furthermore, the data of validating sets should be independent of or different from that of the training sets, which can evaluate the ability of the trained LSTM model to obtain the required output and to verify the calculation accuracy. In this work, the validating set includes two parts: the numerical simulation set and the towing tank test set. The numerical simulation set employed in this work is the data calculated by the software COMPASS-WALCS-NL. The towing tank test set used in this work is the model experimental data obtained in towing tank. Due to the lack of test data of aircraft carrier or destroyer motions, a 15000 TEU container ship is chosen as the research object for test verification[24]. The main dimensions of the target ship are listed in Tab. 1. The representative calculated work conditions chosen in this paper are shown in Tab.2.

Tab. 1 Main dimensions of the 15000 TEU container ship

Principal dimension	Prototype ship
Length overall/m	376
Length waterline /m	357
Breadth /m	46.9
Depth /m	33.9
Draft /m	15.4
Displacement /t	120 721.2

Tab.2 Calculated work conditions

ID	Forward speed U/ kn	Wave height H /m	λ/L	Heading angle β /°
R-I	9	6	1.0	0
R-II		10		
R-III	18	6		
R-IV		10		
R-V	24	3		
R-VI	30			

ID	Forward speed U/ kn	Significant wave height $H_{1/3}$/m	Spectral peak period T_Z/s	Heading angle β /°
IR-I	10	6	9.5	0
IR-II	10	10		
IR-III	14	6		
IR-IV	14	10		

3.1.1 Numerical simulation verification

In this work, the past motion records are taken as input data and the target motions in the future are taken as output data, there is a time difference between the past motions and target motions. The time difference is the predictable time scale that can be obtained from the model. In this sub-section, the predictable time scale is taken as 10 s. Numerical simulation verification in regu-

lar waves is presented in Figs.4–5. The error quantification study is presented in Tab.3. The calculation effect is reflected by the goodness of fit (R^2) and loss function (Loss). The goodness of fit can be written as:

$$R^2 = 1 - \frac{\sum_{i=1}^{n}\left(\hat{y}_i - y_i\right)^2}{\sum_{i=1}^{n}\left(y_i - \bar{Y}\right)^2} \tag{23}$$

where, y_i denotes the actual value, $\hat{y}_i$ denotes the prediction value, and $\bar{Y}$ denotes the mean value. The closer the value of R^2 is to 1, the better the fitting degree is.

Tab.3 Goodness of fit and loss function for numerical verification

Case ID	R^2		Loss	
	Heave	Pitch	Heave	Pitch
R–I	0.9598	0.9477	1.85×10^{-4}	1.96×10^{-4}
R–II	0.9346	0.9312	3.65×10^{-4}	3.89×10^{-4}
R–III	0.9276	0.9221	5.84×10^{-4}	5.15×10^{-4}
R–IV	0.9121	0.9021	6.65×10^{-4}	6.79×10^{-4}

Taking the Fig.4(a) as an example, the data time series consists of two parts: pre–input data and comparative data. The pre–input data represent the original input data required for the operation of motion prediction model, which come from verification data that are obtained by the software COMPASS–WALCS–NL. The span of verification data time series should be the sum of the prediction data time series and the pre–input data time series. In this sub–section, the ratio of pre–input

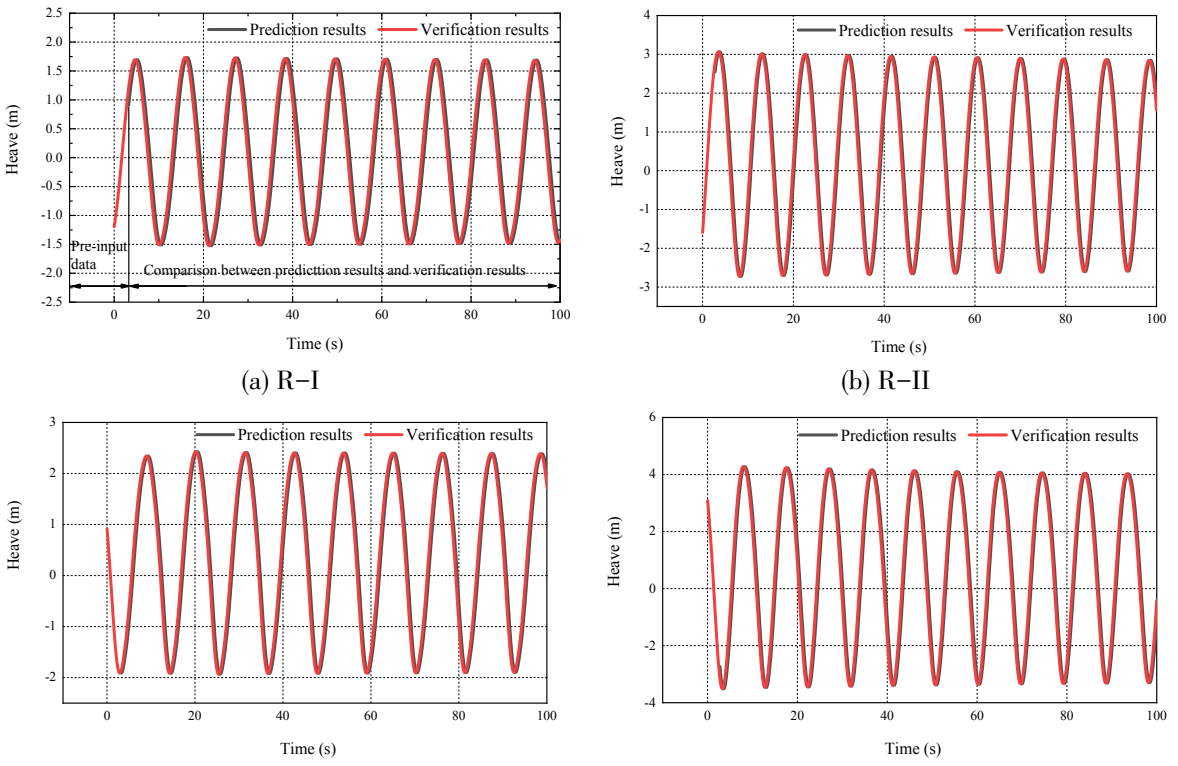

(a) R–I (b) R–II

(c) R–III (d) R–IV

Fig.4 Numerical simulation verification for heave motions

data volume to prediction data volume is 30:1, that is, one target output value can be obtained by 30 pre-input values. And then the time axis continues to move forward until the whole prediction operation is completed.

In addition, it is found from Figs.4-5 that the overall tendencies of the prediction results show good agreement with the experimental results in regular waves. The same tendency can be also found in Tab.3. As shown in Tab.3, all the values of R^2 are larger than 0.9, which means that the proposed method can capture the characteristics of the ship motion responses corresponding to different wave heights, wave frequencies and forward speeds. Furthermore, the calculating accuracy (R^2) of the method decreases as the wave height and forward speed increase. This indicates that as the sea state increases, the complexity of the model also needs to increase, and related training volume and training parameters also need to be adjusted.

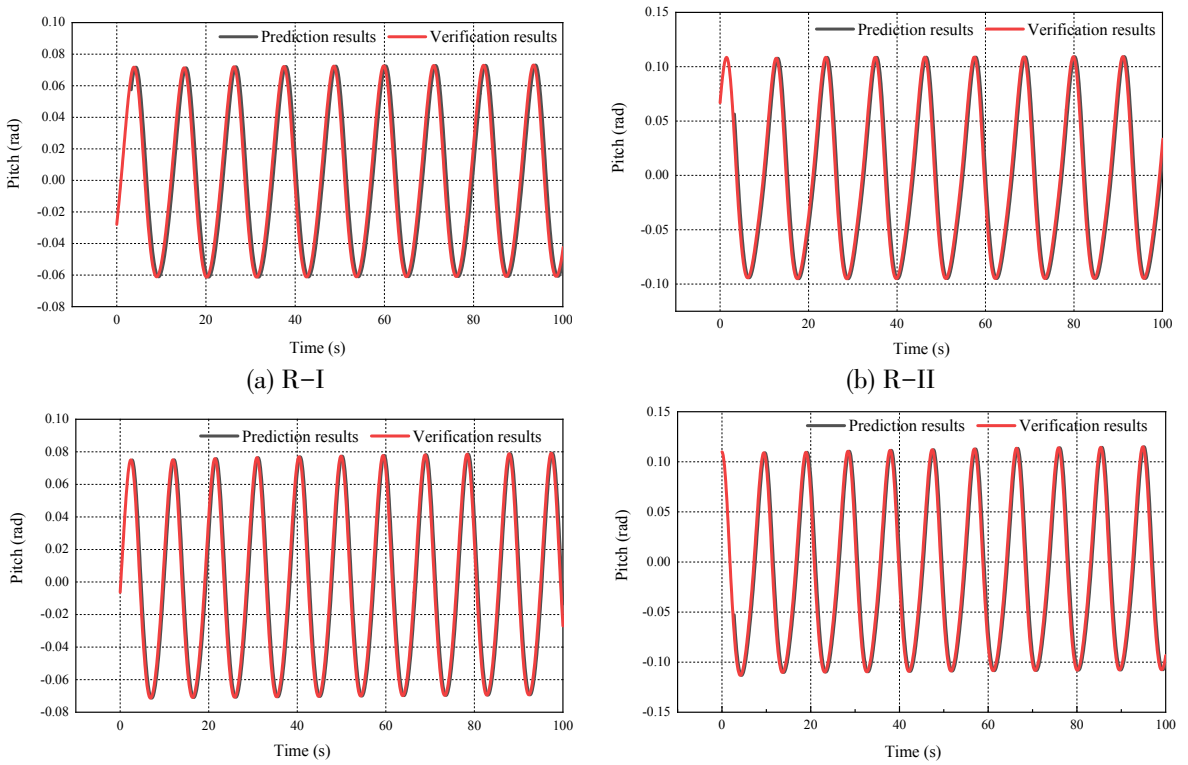

(a) R-I (b) R-II

(c) R-III (d) R-IV

Fig.5 Numerical simulation verification for pitch motions

3.1.2 Towing tank test verification

In addition to the numerical simulation verification, physical test verification is necessary. R-V and R-VI are chosen for the validation of method. The time-domain heave and pitch motions are obtained and compared with the available experimental results[24]. The error quantification study for head wave case is presented in Tab.4. As can be seen from Fig.6, the predicted results are also in good agreement with the experimental data. Moreover, there are subtle differences at the peaks of motion, as shown in Fig.6. Due to the nonlinearity, the sagging values are larger than the hogging values. The value of R^2 obtained based on towing tank tests is lower compared to that in the numerical simulation validation, since the experimental results are disturbed by systematic error. Therefore, the proposed framework can be used in the subsequent simulation of ship motions in irregular waves.

Tab.4 Goodness of fit and loss function for test verification

Case ID	R^2		Loss	
	Heave	Pitch	Heave	Pitch
R- V	0.860	0.898	7.84×10^{-4}	6.95×10^{-4}
R- VI	0.841	0.863	8.01×10^{-4}	7.02×10^{-4}

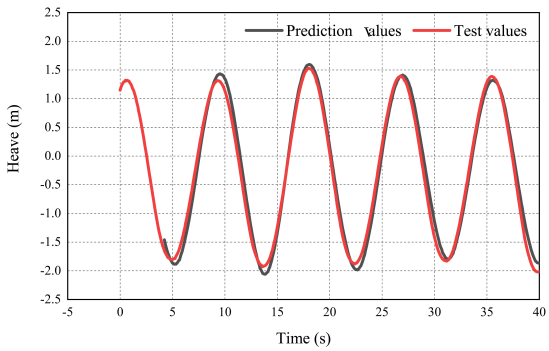

(a) Heave motion at R-V

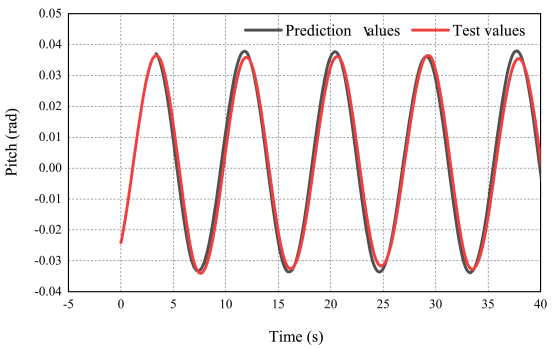

(b) Pitch motion at R-V

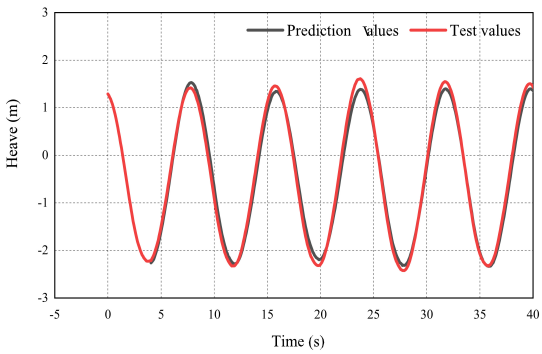

(c) Heave motion at R-VI

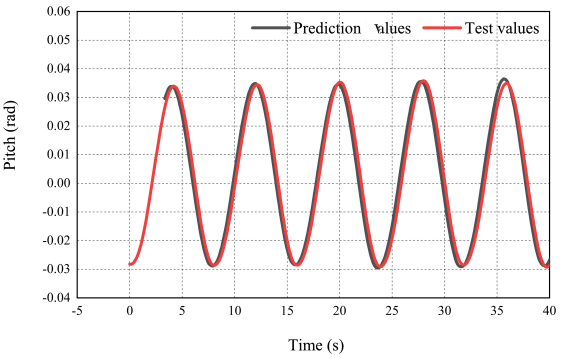

(d) Pitch motion at R-VI

Fig.6 Test verification of ship motions in regular waves

3.2 Data presentation in irregular waves

As concluded from Section 3.1, the prediction model presented in this study effectively meets the precision requirements for regular head waves. However, as actual sea conditions typically involve irregular sea states, the rapid and precise real-time prediction of ship motions for the upcoming seconds in irregular waves holds significant practical importance in the field of ocean engineering. As discussed above, the irregular wave excitation may be regarded as a superposition of a finite number of regular waves at every instant time. For irregular waves, how to study the impact of different wave frequency components on the motion responses is still the key issue and challenge for high accuracy prediction of ship motion. Thus, the wave memory effect needs to be considered.

For various specialized maritime operations, the required time scales are contingent on the specific nature of these operations. For instance, ship-borne helicopter landings necessitate a predictable time scale of 10 seconds, while risk avoidance during ship navigation in waves demands a 30-second time scale. Consequently, the predictable time scales of 10, 30, and 60 seconds for the multi-time scale real-time predictions of ship motions in irregular waves are chosen. To ensure high accuracy in irregular wave conditions, the ratio of pre-input data volume to prediction data volume is set at 45:1.

The time histories of ship motions are depicted in Fig.7, and the error quantification study is detailed in Tab.5. As evidenced by both Fig.7 and Tab.5, prediction accuracy for the three time-scales in irregular waves is notably lower compared to that in regular waves. The decrease in accuracy is not limited to overestimations or underestimations of peak values. It also manifests as frequency dislocations in time series, a departure from the predictability observed in regular wave conditions.

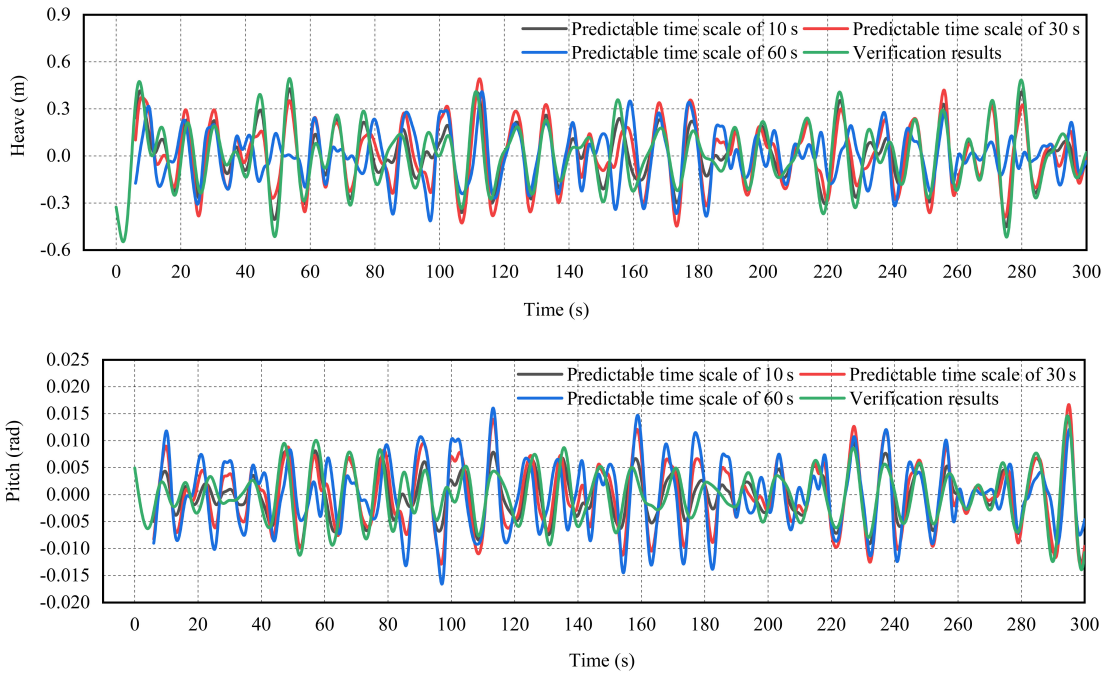

(a) IR-I

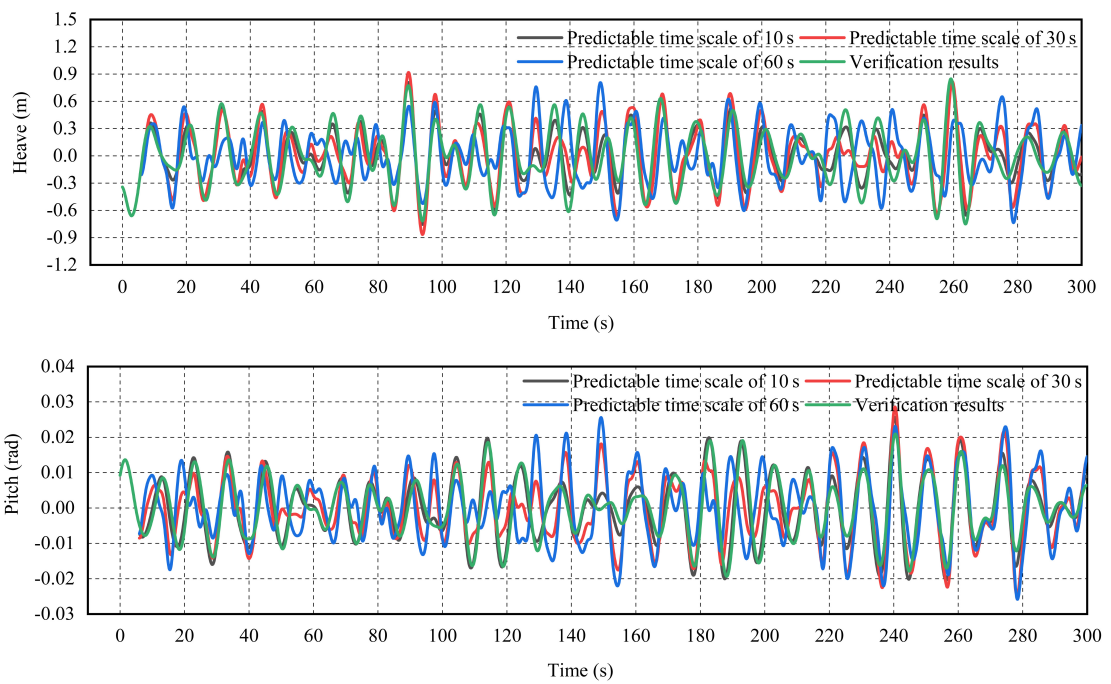

(b) IR-II

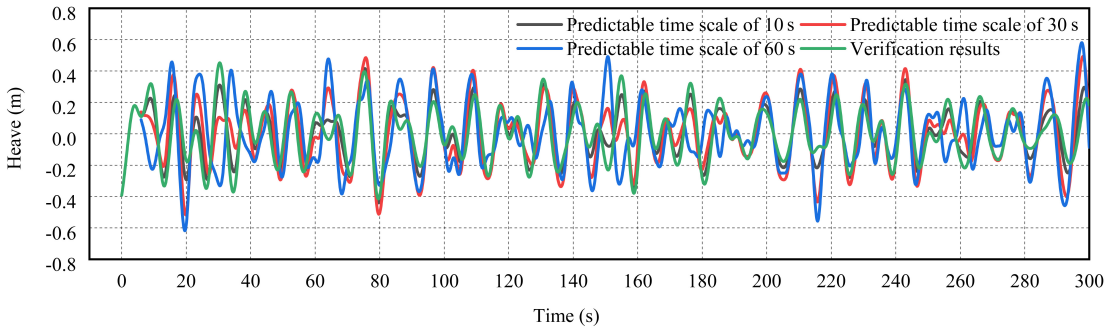

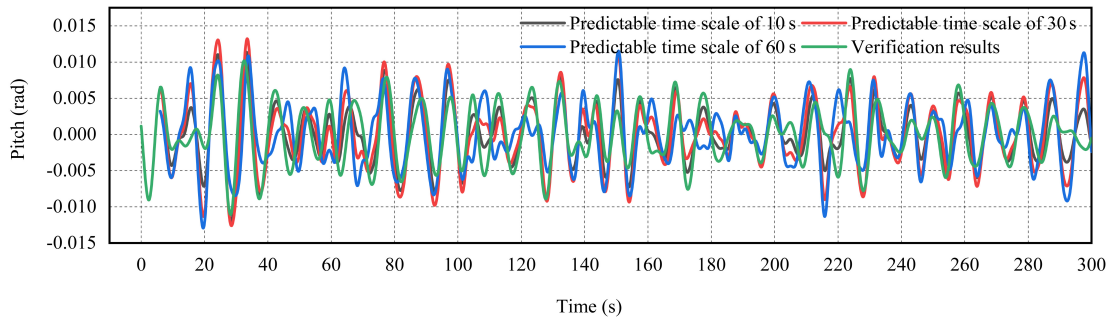

(c) IR-III

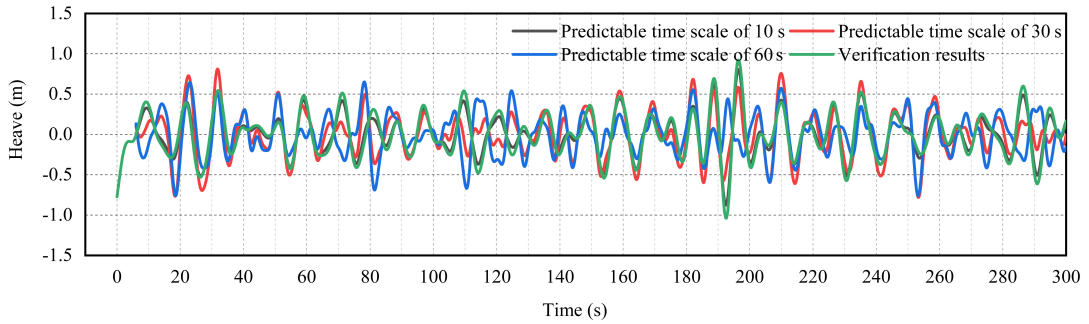

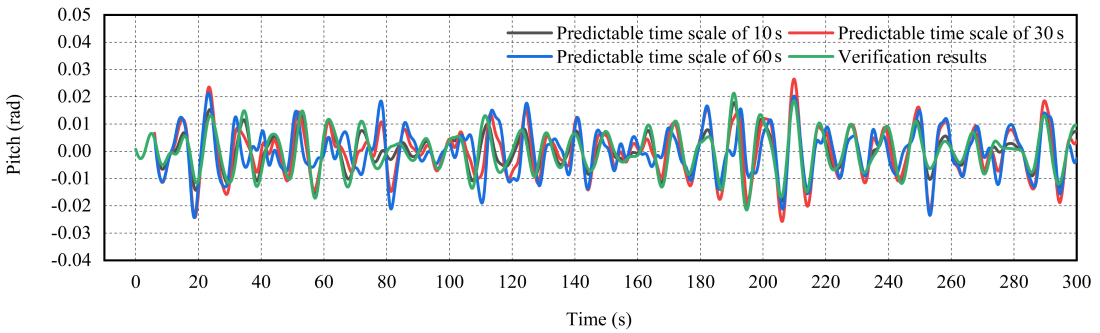

(d) IR-IV

Fig.7 Multi-time scale real-time prediction of ship motions in irregular waves

Tab.5 Goodness of fit and loss function for the condition of irregular waves

Case ID	Predictable time scale	R^2		Loss	
		Heave	Pitch	Heave	Pitch
IR-I	10 s	0.9315	0.9121	6.95×10^{-4}	7.09×10^{-4}
	30 s	0.8894	0.9071	7.75×10^{-4}	7.67×10^{-4}
	60 s	0.8211	0.8318	8.35×10^{-4}	8.25×10^{-4}

Tab.5 (Continued)

Case ID	Predictable time scale	R^2		Loss	
		Heave	Pitch	Heave	Pitch
IR-II	10 s	0.8935	0.8911	7.65×10^{-4}	7.29×10^{-4}
	30 s	0.8084	0.8101	8.05×10^{-4}	8.17×10^{-4}
	60 s	0.7241	0.7388	8.95×10^{-4}	8.88×10^{-4}
IR-III	10 s	0.8375	0.8571	7.85×10^{-4}	7.79×10^{-4}
	30 s	0.7984	0.7801	8.55×10^{-4}	8.57×10^{-4}
	60 s	0.7041	0.7088	9.17×10^{-4}	9.05×10^{-4}
IR-IV	10 s	0.7715	0.7957	8.15×10^{-4}	8.29×10^{-4}
	30 s	0.7064	0.7060	8.95×10^{-4}	8.87×10^{-4}
	60 s	0.6741	0.6918	9.87×10^{-4}	9.75×10^{-4}

4 Concluding remarks

The main highlight of the paper is to propose a framework that can achieve the real-time prediction of ship motions by adopting the LSTM neural network model. Firstly, the basic concepts and training parameters of the LSTM model were introduced. The proposed extreme short time prediction framework for ship motions was a numerical model to realize the numerical prediction of ship motions at the target time based on the known ship motions.

Secondly, combined with the proposed framework in this paper, numerical simulation verification and towing tank test verification studies were carried out, proving that the proposed framework is feasible in simulating nonlinear ship motions.

Finally, the multi-time scale real-time prediction of ship motions in irregular head waves was carried out. The results show that the overall tendencies of the prediction results show good agreement with the numerical verification results. Besides, the prediction accuracy decreases significantly as the predictable time scale increases. The decrease in accuracy is not only reflected in the overestimation or underestimate of peak value, but also in the frequency dislocation of time series.

It is worth mentioning that the study of extreme short-term prediction of nonlinear ship motions in the head irregular waves has been finished. All of these may lay a solid basis for further studies of ship motion prediction in fully random seas (random wave directions, random wave amplitudes and random wave frequencies), and more nonlinear factors will be considered in the future, such as green water.

References

[1] Yang X. Displacement motion prediction of a landing deck for recovery operations of rotary UAVs[J]. Int. J. Contr. Autom. Syst., 2013, 11(1): 58-64.

[2] Huang L, Duan W, Han Y, et al. A review of short-term prediction techniques for ship motions in seaway[J]. J. Ship Mech., 2014, 18(12): 1534-1542.

[3] Akaike H. Fitting autoregressive models for prediction[J]. Annals of the Institute of Statistical Mathematics, 1969, 21: 243-247.

[4] Akaike H. A Bayesian extension of the minimum AIC procedure autoregressive model fitting[J]. Biometrika, 1979, 66: 237-242.

[5] Yumori I R. Real time prediction of ship response to ocean waves using time series analysis[J]. IEEE Oceans, 1981: 1082-1089.

[6] Triantafyllou M, Athans M. Real time estimation of the heaving and pitching motions of a ship using a Kalman filter[C]// IEEE, Boston M A, 1981: 1090-1095.

[7] Triantafyllou M, Bodson M. Real time prediction of marine vessel motion using a Kalman filter techniques[C]//IEEE, Houston, Texas, 1982: 159-165.

[8] Soares C, Cunha C. Bivariate autoregressive models for the time series of significant wave height and mean period[J]. Coastal Engineering. 2000, 40(4): 297-311.

[9] Khan A, Marion K, Bil C. The prediction of ship motions and attitudes using artificial neural networks[J]. Asor Bulletin. 2007, 26(1): 2.

[10] Weng Z, Gu M, Liu C. Extreme short-term prediction of ship motion based on second-order adaptive Volterra series[J]. Journal of Ship Mechanics, 2010, 14(7): 732-740.

[11] Wang K, Li G. DRNN neural network for time series prediction of ship rolling motion[J]. J. Harbin Eng. Univ., 1997, 18: 39-44.

[12] Khan A, Marion K, Bil C. The prediction of ship motions and attitudes using artificial neural networks[J]. ASOR Bulletin, 2008, 26(1): 2-6.

[13] Zhang T, Zheng X, Liu M. Multiscale attention-based LSTM for ship motion prediction[J]. Ocean Engineering. 2021, 230: 109066.

[14] Liu, Y, Duan, W, Huang L, et al. The input vector space optimization for LSTM deep learning model in real-time prediction of ship motions[J]. Ocean Engineering, 2020, 213: 107681.

[15] Gers F, Schmidhuber J, Cummins F. Learning to forget: Continual prediction with LSTM[J]. Neural Computation, 2000, 12 (10): 2451-2471.

[16] Qiao D, Li P, Ma G, et al. Realtime prediction of dynamic mooring lines responses with LSTM neural network model[J]. Ocean Engineering. 2021, 219(2021): 108368.

[17] Sun Q, Tang Z, Gao J, et al. Short-term ship motion attitude prediction based on LSTM and GPR[J]. Applied Ocean Research, 2022, 118: 102927.

[18] Guo X, Zhang X, Tian X, et al. Probabilistic prediction of the heave motions of a semi-submersible by a deep learning model[J]. Ocean Engineering, 2022, 247: 110578.

[19] Cummins W. The impulse response function and ship motions[J]. Schiffstechnik, 1962, 9: 101-109.

[20] Cao Y, A procedure for evaluation, assessment and improvement of added mass and radiation damping of floating structures [C]//Proceedings of the ASME 27th International Conference on Offshore Mechanics and Arctic Engineering, Portugal, 2008: 1-10.

[21] Qiao D, Li P, Ma G, et al.Realtime prediction of dynamic mooring lines responses with LSTM neural network model[J]. Ocean Engineering. 2021, 219: 108368.

[22] Guo X, Zhang X, Tian X, et al. Probabilistic prediction of the heave motions of a semi-submersible by a deep learning model[J]. Ocean Engineering, 2022, 247: 110578.

[23] Boden M. A guide to recurrent neural networks and back propagation[R]. The Dallas Project, 2001: 1-10.

[24] Chen Z, Gui H, Dong P. Nonlinear time-domain hydroelastic analysis for a container ship in regular and irregular head waves by the Rankine panel method[J]. Ships and Offshore Structures, 2019, 14(6): 631-645.

长短期记忆神经网络在船舶迎浪运动多时间尺度实时预测中的应用研究

陈占阳[1,2]，占正勇[3]，常绍平[3]，徐绍峰[3]，刘兴云[1]

（1. 哈尔滨工业大学（威海），山东 威海 264209；2. 大连理工大学工业装备结构分析优化与CAE软件全国重点实验室，辽宁 大连 116024；3. 航空工业西安飞行自动控制研究所，西安 710065）

摘要：波浪引起的船舶运动对海上作业的效率和安全有着重大影响。未来几秒钟内船舶运动的实时预测在执行敏感活动中起着至关重要的作用。然而，船舶运动时间序列具有明显的记忆效应，这给快速准确的预测带来了一定的困难。因此，本文提出了一种基于长短期记忆（LSTM）神经网络模型的实时方法来预测规则/不规则波迎浪中的船舶运动响应。采用15000 TEU集装箱船作为算例模型，对不同时间尺度的不规则波迎浪中船舶运动响应进行了数值预报和实时预测，并利用相关试验数据对结果进行了验证。结果表明，在非线性船舶运动预测中，所提出的方法比基于势流理论的经典极值短期预报更具可信度。

关键词：深度学习；LSTM；船舶运动；实时预报；不规则波

中图分类号：U661.32　　**文献标识码：**A

基金项目：山东省自然科学基金面上项目（ZR2024ME139）；航空科学基金（2024M074189001）；工业装备结构分析国家重点实验室开放基金资助项目（GZ23112）

作者简介：陈占阳（1984-），男，博士，哈尔滨工业大学（威海）副教授；

占正勇（1975-），男，博士，航空工业西安飞行自动控制研究所副总工程师；

常绍平（1992-），男，硕士，航空工业西安飞行自动控制研究所工程师；

徐绍峰（1999-），男，硕士研究生；

刘兴云（2000-），男，硕士研究生。